CWI Quarterly
Volume 10 (3&4) 1997, pp. 215 – 238

Boundary Layer-Adapted Grids and Domain Decomposition in Stabilized Galerkin Methods for Elliptic Problems

R. Hangleiter and G. Lube
University of Göttingen,
Mathematics Department, D–37083 Göttingen
e-mail: lube@math.uni-goettingen.de

Global error estimates are considered for stabilized Galerkin finite element methods to second order elliptic boundary value problems with emphasis on the singularly perturbed case. We address the resolution of boundary layers on layer-adapted grids using both anisotropic interpolation estimates and sharp estimates of derivatives. A critical point is the choice of numerical damping parameters. A non-overlapping domain decomposition method is considered for an efficient solution of the discrete problems.

1. Introduction

We apply stabilized Galerkin finite element methods to elliptic boundary value problems of second order (advection-diffusion-reaction model), with emphasis on singularly perturbed problems. Such problems appear e.g. within the iterative solution of coupled incompressible Navier-Stokes problems [5], [16].

The Galerkin method may suffer from numerical instabilities generated by dominant advection/ reaction. Hughes et al. introduced the concept of *stabilized* Galerkin methods which combine improved stability and accuracy due to a residual formulation. The numerical analysis of such methods is more or less restricted to *quasi-uniform meshes* so far, but in the singularly perturbed case it is often desirable to resolve boundary or interior layers [20], [21].

The outline of this paper is as follows: In Section 2 we review a class of *stabilized Galerkin methods*, derive a basic quasi-optimal estimate and give a-priori error estimates on quasi-uniform meshes. In the singularly perturbed case, we try to resolve boundary layers. A modified application of the quasi-optimal estimate using asymptotic expansions is addressed in Section 3 for

a 2D model in combination with a-priori generation of layer-adapted grids and (anisotropic) interpolation estimates for exponentially decaying boundary layers (cf. Section 4). In Section 5 we present a non-overlapping domain decomposition method, with application to numerical experiments.

For a subdomain $G \subseteq \Omega$ we denote by $W^{k,p}(G)$ the usual Sobolev space of functions with derivatives of order $\leq k$ belonging to $L^p(G)$. The norm resp. seminorm on $W^{k,p}(G)$ are denoted by $\|\cdot\|_{k,p,G}$ resp. $|\cdot|_{k,p,G}$. $(\cdot,\cdot)_G$ is the inner product in $L^2(G)$. In case of $G = \Omega$ we usually omit the index Ω. C denotes a generic constant not depending on singular perturbation and discretization parameters.

2. Stabilized Galerkin Methods

2.1. Continuous problem

Consider the following *elliptic boundary value problem*

$$L_\varepsilon u := -\varepsilon \Delta u + \mathbf{b} \cdot \nabla u + cu = f \quad \text{in } \Omega \tag{1}$$

$$u = 0 \quad \text{on } \partial\Omega \tag{2}$$

on a bounded domain $\Omega \subset \mathbf{R}^d, d \leq 3$ with a Lipschitzian boundary $\partial\Omega$ and outer normal $\mathbf{n}$.

Of particular interest is the *singularly perturbed* case $0 < \varepsilon \ll 1$ where the solution of (1)-(2) is mainly characterized by the solution u_0 of the limit problem for $\varepsilon = 0$. Different kinds of interior resp. boundary layers of the solution of (1)-(2) can appear in subregions where u_0 is not smooth resp. where u_0 does not satisfy (2). In particular, boundary layers may appear at outflow parts Γ_+ of $\partial\Omega$ where $\mathbf{b} \cdot \mathbf{n} > 0$ or at characteristic parts Γ_0 with $\mathbf{b} \cdot \mathbf{n} = 0$.

Throughout this paper, we assume for problem (1)-(2):

(H.1a) $\quad 0 < \varepsilon \leq 1, \quad \mathbf{b} \in W^{1,\infty}(\Omega)^d, \quad c \in L^\infty(\Omega), \quad f \in L^2(\Omega)$

(H.1b) $\quad c \geq 0, \quad \nabla \cdot \mathbf{b} = 0 \quad$ a.e. in Ω .

A *weak solution* $u \in V := W_0^{1,2}(\Omega)$ of (1)-(2) satisfies

$$\text{Find } u \in V \text{ such that: } \; B_G(u,v) = (f,v), \quad \forall v \in V \tag{3}$$

$$B_G(u,v) := (\varepsilon \nabla u, \nabla v) + \frac{1}{2}\left((\mathbf{b} \cdot \nabla u, v) - (\mathbf{b} \cdot \nabla v, u)\right) + (c\, u, v) \tag{4}$$

(using integration by parts of the advective term). The standard *energy norm* reads

$$|||v|||_G := \sqrt{B_G(v,v)} := \left(\varepsilon |v|_{1,2,\Omega}^2 + \|\sqrt{c} v\|_{0,2,\Omega}^2\right)^{1/2}. \tag{5}$$

2.2. Stabilized Galerkin methods

We consider Lagrangian elements on simplices $K \subset \mathbf{R}^d$ of an admissible triangulation $\mathcal{T}_h = \{K\}$ with $\overline{\Omega} = \cup_K \overline{K}$. $\Pi_l(K)$ is the set of polynomials of maximal degree $l \geq 1$ on K. The Lagrangian interpolant of a continuous function v is uniquely determined by $(I_h^{(l)} v)(x_i) = v(x_i)$ for all nodal points of K.

Let $V_h \subset V$ be the finite–dimensional subspace of conforming finite elements such that $V_h|_K \subset \Pi_l(K)$. The *standard Galerkin method* reads

$$\text{Find } u_h \in V_h \text{ such that}: \quad B_G(u_h, v_h) = (f, v_h), \quad \forall v_h \in V_h. \tag{6}$$

For later extension on possibly different sizes of the element in different directions, we introduce some *notation*, cf. Figure 1: For $K \subset \mathbf{R}^2$ let E_K be the longest edge of K. Then we denote by $h_{1,K} := \text{meas}(E_K)$ its length and by $h_{2,K} := 2\text{meas}(K)/h_{1,K}$ the diameter of K perpendicularly to E_K.

In the 3D-case we proceed as follows. Let again E_K be the longest edge of K, and let F_K be the larger of the two faces of K with $E_K \subset \overline{F}_K$. Then we denote by $h_{1,K} := \text{meas}(E_K)$ the length of E_K, by $h_{2,K} := 2\text{meas}(F_K)/h_{1,K}$ the diameter of F_K perpendicularly to E_K, and by $h_{3,K} := 6\text{meas}(K)/(h_{1,K}h_{2,K})$ the diameter of K perpendicularly to F_K. Then holds $h_{1,K} \geq .... \geq h_{d,K}$. Later on, an element K will be called *isotropic* if $h_{1,K} \approx h_{d,K}$ resp. *anisotropic* if $h_{1,K} \gg h_{d,K}$.

Throughout this paper, for interpolation estimates on an element K we require the

MAXIMAL ANGLE CONDITION. *There is a constant $\gamma^* < \pi$ (independent of h and $K \in \mathcal{T}_h$) s.t. the maximal interior angle γ_K of any element K is bounded by $\gamma^* : \ \gamma_K \leq \gamma^*$.*

The 3D-condition can be formulated by analogy [3]. Then we have with $\eta_u := u - I_h^{(l)} u$ the following interpolation result on *arbitrary* elements:

$$\forall u \in W^{l+1,2}(K) : \ ||\eta_u||_{m,2,K} \leq C h_{1,K}^{l+1-m} |u|_{l+1,2,k} \quad 0 \leq m \leq l+1, \ \forall K \in \mathcal{T}_h. \tag{7}$$

In the singularly perturbed case $0 < \varepsilon \ll 1$, it is often useful to stabilize unphysical oscillations of the discrete Galerkin solution. Using that under assumptions (H.1) a solution $u \in V$ satisfies $L_\varepsilon u = f$ in $L^2(\Omega)$, we consider *stabilized Galerkin methods* of residual type

$$\text{Find } U_h \in V_h \ \text{ such that } \ B_{SG}(U_h, v) = F_{SG}(v) \quad \forall v \in V_h \tag{8}$$

$$\begin{aligned} B_{SG}(v, w) &:= B_G(v, w) + \sum_K (L_\varepsilon v, \psi(w))_K ; \\ F_{SG}(w) &:= f(w) + \sum_K (f, \psi(w))_K , \end{aligned} \tag{9}$$

$$\psi(v_h)|_K := \delta_K (\mathbf{b} \cdot \nabla) v_h + \gamma_K (-\varepsilon \Delta v_h + c v_h) \in L^2(K), \tag{10}$$

with $0 \leq |\gamma_K| \leq \delta_K$, a unique sign of all γ_K and the following *minimal design properties*

(H.2) $\exists\theta \in (0,\Theta):\ (i)\ \varepsilon\delta_K C_I^2 \le \frac{\theta}{2} h_{d,K}^2\ ;\quad (ii)\ \delta_K c \le \frac{\theta}{2}$ a.e. in Ω

where $\Theta = 3$ if $\inf_K \gamma_K \ge 0$ and $\Theta = \frac{1}{2}$ if $\sup_K \gamma_K \le 0$. The constant C_I (with $C_I = 0$ if $l = 1$) appears from the inverse inequality

$$||\Delta v||_{0,2,K} \le C_I h_{d,K}^{-1} |v|_{1,2,K} \quad \forall v \in V_h.$$

Assumption (H.2) covers in particular

- the *streamline upwind method (SUPG)* with $\delta_K \ge 0,\ \gamma_K = 0$,

- the *Galerkin/ Least-squares method (GLS)* with $\delta_K = \gamma_K \ge 0$ and

- the *Douglas–Wang method* with $\delta_K = -\gamma_K \ge 0$.

The Galerkin approach corresponds to $\delta_K = \gamma_K \equiv 0$. The *critical point* is the choice of the sets $\{\delta_K\}$ and $\{\gamma_K\}$ such that (8)-(10) yields a stable and accurate method.

2.3. Quasi-optimal energy norm estimates on arbitrary grids

We introduce the following *stabilized energy norm* $|||\cdot|||_{SG}$ defined by

$$\begin{aligned} |||v|||_{SG}^2 &:= |||v|||_G^2 + \sum_K \delta_K ||\mathbf{b}\cdot\nabla v||_{0,2;K}^2 + \\ &+ \sum_K \max(0;\mathrm{sgn}(\gamma_K)) || - \varepsilon\Delta v + cv||_{0,2;K}^2 \end{aligned} \tag{11}$$

and

$$T_\delta^{SS}(v) := \sum_K \delta_K ||\mathbf{b}\cdot\nabla v||_{0,2;K}^2;\ \ T_{|\gamma|}^S(v) := \sum_K |\gamma_K|\ || - \varepsilon\Delta v + cv||_{0,2;K}^2. \tag{12}$$

Additional stability of the skew-symmetric part of the operator (or weighted control of the streamline derivative) is the *main effect* of the stabilization. We start with the following more or less standard stability and continuity estimates, cf. [9], [19], [21].

LEMMA 2.1. *For $v_h \in V_h$ we obtain under the assumptions (H.1), (H.2):*

$$B_{SG}(v_h, v_h) \ge C_0(\theta) |||v_h|||_{SG}^2 \tag{13}$$

with $C_0(\theta) = 1 - \frac{\sqrt{1+\theta}}{2}$ if $\inf_K \gamma_K \ge 0$ and $C_0(\theta) = 1 - \alpha(\theta)$, $\alpha(\theta) = \frac{1}{2}(\theta + \sqrt{\theta^2 + 4\theta})$ if $\sup_K \gamma_K \le 0$. Consequently, the stabilized schemes (8)-(10) are uniquely solvable.

Now we introduce the notation

$$B_K := ||\mathbf{b}||_{0,\infty,K}, \quad C_K := ||c||_{0,\infty,K}, \quad Z_K := \min\left(\delta_K^{-1}; B_K^2 \varepsilon^{-1}\right). \tag{14}$$

LEMMA 2.2. *For $u \in V$ with $\Delta u \in L^2(K), \forall K \in \mathcal{T}_h$ and $v \in V_h$ we obtain under the assumptions (H.1), (H.2) that*

$$|B_{SG}(u,v)| \leq \frac{C_0(\theta)}{2}|||v|||_{SG}^2 + \frac{\tilde{K}}{2C_0(\theta)}Q_{SG}(u), \tag{15}$$

$$Q_{SG}(u) := |||u|||_G^2 + T_\delta^{SS}(u) + T_{|\delta|}^S(u) + \sum_K Z_K \|u\|_{0,2,K}^2 \tag{16}$$

with $\tilde{K} = 3$ if $\inf_K \gamma_K \geq 0$ resp. $\tilde{K} = 6$ if $\sup_K \gamma_K \leq 0$ and the obvious definition of $T_{|\delta|}^S(\cdot)$, cf. (12).

For the stabilized methods (8)-(10), then we have the following variant of Cea's Lemma.

THEOREM 2.3. *The assumptions (H.1)–(H.2) imply the quasi–optimal a-priori error estimate of the stabilized Galerkin methods (8)-(10)*

$$|||u - U_h|||_{SG} \leq C\ Q_{SG}(u - I_h^{(l)}u) \tag{17}$$

where C denotes a constant which is independent of ε, h, δ_K, and γ_K. Note that in particular $Q_{SG}(v) := |||v|||_G$ and $C = 1$ if $\delta_K = \gamma_K \equiv 0$, $\mathbf{b} = \mathbf{0}$.

PROOF. Let

$$e_h := U_h - u = (U_h - I_h^{(l)}u) + (I_h^{(l)}u - u) \equiv \chi_h + \eta_h$$

where $I_h^{(l)} : V \to V_h$ denotes the Lagrangian interpolation operator. By Lemma 2.1, Lemma 2.2 and the consistency of the methods, we obtain

$$\begin{aligned} C_0|||\chi_h|||_{SG}^2 &\leq B_{SG}(\chi_h,\chi_h) = B_{SG}(e_h - \eta_h, \chi_h) = -B_{SG}(\eta_h,\chi_h) \\ \leq \frac{C_0}{2}|||\chi_h|||_{SG}^2 &+ \\ + \frac{K}{2C_0} &\left(|||\eta_h|||_G^2 + T_\delta^{SS}(\eta_h) + T_{|\delta|}^S(\eta_h) + \sum_K Z_K \|\eta_h\|_{0,2,K}^2 \right). \end{aligned}$$

The triangle inequality and (16) conclude the proof. □

2.4. Energy norm stimates on quasi-uniform grids

Now we give an error estimate on *quasi–uniform grids* where $h_K \approx h_{1,K} \approx h_{d,K}$ and determine the parameters δ_K and γ_K. Note that we introduce (with respect to the anisotropic case in Section 4) a *modified* definition of the *mesh Péclet number*

$$Pe_K := h_{d,K} B_K \varepsilon^{-1}. \tag{18}$$

THEOREM 2.4. *Let the solution of (1)-(2) be smooth according to $u \in V \cap W^{l+1,2}(\Omega)$ and the triangulation $\mathcal{T}_h$ quasi-uniform such that for each element K holds $h_K := h_{1,K} \approx h_{d,K}$. Then, under the assumptions (H.1)-(H.2) and with the choice*

$$|\gamma_K| \le \delta_K \sim \min\left(h_{d,K}B_K^{-1}; h_{d,K}^2\varepsilon^{-1}\right), \tag{19}$$

the a-priori discretization error estimate of the stabilized Galerkin methods reads

$$|||u-U_h|||_{SG}^2 \le C\sum_K h_K^{2l}\left(\varepsilon + B_K h_K + C_K h_K^2\right)|u|_{l+1,2,K}^2. \tag{20}$$

PROOF From Theorem 2.3 and the approximation result (7) we conclude using (H.2)(ii)

$$\begin{aligned} |||e_h|||_{SG}^2 &\le C\left(|||\eta_h|||_G^2 + T_\delta^{SS}(\eta_h) + T_{|\delta|}^S(\eta_h) + \sum_K Z_K\|\eta_h\|_{0,2,K}^2\right) \\ &\le C\sum_K h_{1,K}^{2l}\left(\varepsilon + C_K h_{1,K}^2 + \delta_K B_K^2 + Z_K h_{1,K}^2\right)|u|_{l+1,2,K}^2. \end{aligned} \tag{21}$$

Balancing the terms $\delta_K B_K^2 \sim Z_K h_{1,K}^2 = h_{1,K}^2 \min\left(\delta_K^{-1}; B_K^2\varepsilon^{-1}\right)$, we arrive with the mesh Peclet number as in (18) at $\delta_K \sim h_{d,K}B_K^{-1}$ if $Pe_K \ge 1$ and $\delta_K \sim h_{d,K}^2\varepsilon^{-1}$ if $Pe_K \le 1$. Note that this definition gives no contradiction to (H.2). This concludes the proof. □

REMARK 2.5. (i) In the *weakly anisotropic case* $h_{1,K}/h_{d,K} =: \Gamma_K \le \Gamma$ for all $K \in \mathcal{T}_h$ such that $\Gamma \not\gg 1$ which allows for local mesh-refinement, we have the modified estimate

$$|||u-U_h|||_{SG} \le C\sum_K h_K^{2l}\left(\varepsilon + \Gamma_K B_K h_K + C_K h_K^2\right)|u|_{l+1,2,K}^2. \tag{22}$$

(ii) In contrast to other papers (e.g. [7], [15]), we did not include the reaction term in the design of the parameters δ_K and γ_K. The main point is that, in the *symmetric case* the quasi-optimal estimate in the energy norm $|||\cdot|||_G$ with the optimal constant $C = 1$ of the Galerkin method cannot be improved. For linear elements, it is wrong to use the GLS method, as numerical dissipation is then substracted instead of being added to the Galerkin method. We did not find an improvement with the Douglas-Wang variant in numerical experiments [2].

3. Asymptotic Expansion of the Continuous Problem

In the singularly perturbed case $0 < \varepsilon \ll 1$, the estimates of Theorem 2.4 are in general not satisfactory. The interpolation estimate in (17) requires information on local Sobolev norms of the solution which are in general not uniformly bounded with respect to $\varepsilon \to +0$.

Stabilized Galerkin methods have the advantage of high accuracy away from boundary and interior layers where the solution is smooth [22], [13]. Different methods have been proposed to remedy (restricted) oscillations of the discrete solutions of stabilized Galerkin methods in layer regions, e.g. methods of shock-capturing type [4] or methods using stabilizing terms of higher order [8], [24]. Such methods are in general not satisfactory to resolve layers.

In the remainder of this paper, we combine stabilized Galerkin methods with the *resolution of layers* (as important point in practical computations). Therefore we modify the application of the quasi–optimal estimate of Theorem 2.3 using the asymptotic expansion $u = u_M^{as} + r_M$ with a sufficiently small remainder r_M:

$$|||u - U_h|||_{SG} \leq C\{Q_{SG}(u_M^{as} - I_h^{(l)} u_M^{as}) + Q_{SG}(r_M - I_h^{(l)} r_M)\}. \tag{23}$$

It is often possible to find estimates of the derivatives of the asymptotic expansion. On the other hand, we require only a low order estimate of the remainder.

3.1. Asymptotic expansion of the solution

The behaviour of the solution of (1)-(2) with $0 < \varepsilon \ll 1$ can be arbitrarily complicated, depending essentially on the behaviour of the characteristics of the limit operator L_0. So we restrict ourselves to the model problem (1)-(2) on a bounded polygonal and convex domain Ω, with sufficiently smooth data and with a "simple" asymptotic structure of the solution. The precise assumptions will be given below. In particular, interior layers and geometrical singularities at corners are avoided. Moreover assume that for any edge $\Sigma \subset \partial\Omega$ holds

(H.3) $\quad \Sigma \subseteq \Gamma_\pm$ with $|\mathbf{b} \cdot \mathbf{n}||_\Sigma \geq \beta > 0 \quad$ or $\quad \Sigma \subseteq \Gamma_0$, i.e. $\mathbf{b} \cdot \mathbf{n}|_\Sigma \equiv 0$.

This considerably simplifies the different possibilities of boundary layer behaviour at $\Gamma_+ \cup \Gamma_0$.

A standard expansion of the solution of (1)-(2) without interior layers has the structure

$$u \;=\; u_M^{as} + \;\; r_M \;\equiv\; (U_M \;+\; V_M \;+\; Z_M) \;\;+\;\; r_M \tag{24}$$

with the *global (regular) expansion* U_M, *boundary layer* expansions V_M (of outflow or characteristic type), *corner layer* expansions Z_M at corners, if there holds $V_M + U_M \neq 0$, and the remainder r_M, cf. [21], [10]. The global part $U_M := \sum_{j=0}^{M} \varepsilon^j u_j(x)$ solves recursively the system

$$L_0 u_j := \mathbf{b} \cdot \nabla u_j + c u_j = f_j \;\text{ in }\; \overline{\Omega} \setminus \Gamma_-; \;\; u_j = 0 \;\text{ on }\; \Gamma_-; \;\; j = 0, ..., M \tag{25}$$

with $f_0 = f$ and $f_j := \Delta u_{j-1}, j = 1, ..., M$. Let us assume now that

(H.4) $\quad U_M \in W^{l+1,\infty}(\Omega)$.

In particular, no interior layer originates at points of $\overline{\Gamma}_- \cap \overline{\Gamma_+ \cup \Gamma_0}$. (Isotropic) interpolation estimates of U_M and the design of the sets $\{\gamma_K\}$, $\{\delta_K\}$, as given in (19), follow now similarly as in Theorem 2.4 for subdomains away from layer regions.

3.2. Construction of boundary layer corrections

The global expansion U_M does in general not satisfy the boundary conditions (2) at outflow resp. characteristic boundaries Γ_+ resp. Γ_0. According to (H.3), an edge $\Sigma \subset \partial\Omega\backslash\Gamma_-$ belongs either to Γ_+ or Γ_0. We introduce a local coordinate system (ϕ, ρ) in a neighborhood $\mathcal{U}(\Sigma)$ of Σ where $\rho(x) := \mathrm{dist}(x, \Sigma)$ and ϕ denotes a tangential variable on Σ. The diffeomorphic mapping $(x_1, x_2) \mapsto (\phi, \rho)$ transforms the operator L_ε to

$$\tilde{L}_\varepsilon u := -\varepsilon \tilde{L}_2 u + \tilde{L}_0 u \equiv -\varepsilon \left(A \frac{\partial^2 u}{\partial \rho^2} + \hat{L}_2^R u \right) + \left(B_1 \frac{\partial u}{\partial \phi} + B_2 \frac{\partial u}{\partial \rho} + B_0 u \right), \quad (26)$$

with $A(\phi, \rho) := \sum_{i=1}^{2} \left(\frac{\partial \rho}{\partial x_i} \right)^2 > 0$; $B_1(\phi, \rho) := \mathbf{b} \cdot \nabla \phi$,
$B_2(\phi, \rho) := \mathbf{b} \cdot \nabla \rho$, $B_0(\phi, \rho) := c$. Taylor expansion of the coefficients at $\rho = 0$ yields

$$\begin{aligned} A(\phi, \rho) &= \sum_{i=0}^{K} A_i(\phi) \rho^i + o(|\rho|^K), \\ B_j(\phi, \rho) &= \sum_{i=0}^{K} B_{j,i}(\phi) \rho^i + o(|\rho|^K), \quad j = 0, 1, 2. \end{aligned} \quad (27)$$

Introducing the transformation $\zeta := \rho / \varepsilon^\sigma$, we determine $\sigma \in (0, 1]$ such that

$$\frac{||\varepsilon(\tilde{L}_2 v)(\phi, \varepsilon^\sigma \zeta)||_{0,\infty,\mathcal{U}}}{||(\tilde{L}_0 v)(\phi, \varepsilon^\sigma \zeta)||_{0,\infty,\mathcal{U}}} = \mathcal{O}_s(1), \quad \varepsilon \to 0. \quad (28)$$

3.2.1. Outflow layers.

The simplest case appears if Σ is part of the *outflow boundary* Γ_+ such that $B_{2,0}(\phi) = \mathbf{b} \cdot \nabla \rho|_{\rho=0} = \mathbf{b} \cdot \mathbf{n}|_\Sigma \geq \beta > 0$. Then (28) results in $\sigma = 1$ and (with $K := M$)

$$L_\varepsilon \to \tilde{L}_\varepsilon := \frac{1}{\varepsilon} \sum_{j=0}^{M} L_j^+(\phi, \zeta) \varepsilon^j + \ldots \text{ h.o.t. } \ldots, \qquad L_0^+ := -A_0 \frac{\partial^2}{\partial \zeta^2} + B_{2,0} \frac{\partial}{\partial \zeta}.$$

The formal expansion of the boundary layer correction $V_M := \sum_{j=0}^{M} v_j^+(\phi, \zeta)$ can then be determined recursively from the system of *ordinary* differential equations

$$L_0^+ v_0^+ = 0; \qquad L_0^+ v_j^+ = -\sum_{k=1}^{j} L_k^+ v_{j-k}^+, \quad j = 1, \ldots, M \qquad \text{in } \mathcal{U}(\Sigma)$$

with $v_j^+ + u_j = 0$ on Σ. We obtain sufficiently smooth solutions (via smoothness of the data and of U_M) of *exponentially decaying* form

$$v_j^+(\phi, \zeta) = \exp\left(\frac{-B_{2,0}(\phi)\zeta}{A_0(\phi)} \right) \sum_{i=0}^{I(j)} c_{ij}(\phi) \zeta^i.$$

3.2.2. Characteristic layers
Assume now that an edge Σ belongs to Γ_0, hence $B_{2,0}(\phi) = \mathbf{b} \cdot \nabla\rho|_{\rho=0} = \mathbf{b}\cdot\mathbf{n}|_\Sigma \equiv 0$. Let k_j be the smallest index in (27) such that $B_{j,k_j} \not\equiv 0$. We restrict ourselves to the simplest variants: Under one of the assumptions $c(x)|_\Sigma = B_0(\phi) \geq \gamma > 0$ or $|B_{1,0}(\phi)| = |\mathbf{b} \cdot \nabla\phi|_\Sigma| \geq \gamma > 0$, (28) yields $\sigma = 1/2$. This implies with $K = 2M$ that

$$L_\varepsilon \to \tilde{L}_\varepsilon := \sum_{j=0}^{2M} L_j^0(\phi,\zeta)\varepsilon^{j/2};$$
$$L_0^0 := -A_0\frac{\partial^2}{\partial\zeta^2} + B_{1,0}\frac{\partial}{\partial\phi} + B_{2,1}\zeta\frac{\partial}{\partial\zeta} + B_{0,0}I.$$

(i) Reaction-diffusion problems: The simplest case appears in (29) if $\mathbf{b} \equiv \mathbf{0}$ and $c \geq \gamma > 0$, hence $k_1 = k_2 = \infty$ and $L_0^0 := -A_0\frac{\partial^2}{\partial\zeta^2} + B_{0,0}I$. The formal expansion of the layer correction $V_M := \sum_{j=0}^{2M} v_{j/2}^0(\phi,\zeta)$ can then be determined recursively from *ordinary* differential equations

$$L_0^0 v_0^0 = 0, L_0^0 v_j^0 = -\sum_{k=1}^{j} L_k^0 v_{j-k}^0,\ j = 1,...,2M \qquad \text{in } \mathcal{U}(\Sigma),$$

and $v_{2j}^0 + u_j = 0, j = 0,...,K$; $v_{2j-1}^0 = 0, j = 1,...,M$ on Σ with *exponentially decaying solutions*

$$v_j^0(\phi,\zeta) = \exp\left(\frac{-B_{0,0}(\phi)\zeta}{A_0(\phi)}\right)\sum_{i=0}^{I(j)} c_{ij}(\phi)\zeta^i.$$

(ii) Advection-diffusion problems: (29) is more complicated if $\mathbf{b} \not\equiv \mathbf{0}$, $\mathbf{b}\cdot\mathbf{n} = 0$ at Γ_0 and $\min_{j=1,2} k_j$ is finite. The simplest case appears for $k_1 = 0, k_2 \geq 2$, hence $L_0^0 := -A_0\frac{\partial^2}{\partial\zeta^2} + B_{1,0}\frac{\partial}{\partial\phi} + B_{0,0}I$. The formal expansion of the correction $V_M := \sum_{j=0}^{2M} v_{j/2}^0(\phi,\zeta)$ can then be determined recursively from *parabolic* differential equations

$$L_0^0 v_0^0 = f_0^0 := 0, \qquad L_0^0 v_j^0 = f_j^0 := -\sum_{k=1}^{j} L_k^0 v_{j-k}^0,\ j = 1,...,2M \qquad \text{in } \mathcal{U}(\Sigma)$$

such that $U_M + V_M$ satisfies (2) on Σ (i.e. at $\rho = 0$) resp. at $\phi = 0$. A smooth transformation

$$\phi \mapsto \tilde{\phi} := H(\phi) = \int_0^\phi \frac{A_0(\tau)}{B_{1,0}(\tau)}\,d\tau, \qquad \tilde{v}_j := v_j \exp\left(\int_0^\phi \frac{B_{0,0}(\tau)}{B_{1,0}(\tau)}\,d\tau\right).$$

results in

$$\tilde{L}_0^0\tilde{v}_j^0 := -\frac{\partial^2\tilde{v}_j^0}{\partial\zeta^2} + \frac{\partial\tilde{v}_j^0}{\partial\tilde{\phi}} = \tilde{f}_j^0 := \frac{1}{A_0}f_j^0 \exp\left(\int_0^\phi \frac{B_{0,0}(\tau)}{B_{1,0}(\tau)}\,d\tau\right).$$

The leading term has the form

$$\tilde{v}_0^0 := -\sqrt{\frac{2}{\pi}} \int_{\zeta/\sqrt{2\tilde{\phi}}}^{\infty} \exp\left(-\frac{1}{2}t^2\right) u_0\left(\tilde{\phi} - \frac{\zeta^2}{2t}\right)\, dt. \tag{29}$$

Corresponding expressions can be found for higher order terms $\tilde{v}_j^0$ of the layer expansion. The terms $\tilde{v}_j^0$ resp. v_j^0 are sufficiently smooth under (rather restrictive) *compatibility conditions*

$$\frac{\partial^k u_j}{\partial \phi^k} = 0, \quad |k| \le l \qquad \text{at } \phi = 0 \quad \text{(resp. at } \Sigma \cap \Gamma_-\text{)}. \tag{30}$$

REMARK 3.1. The structure of the layer terms arising from (26) can be much more complicated in other cases of the numbers k_j as discussed above, cf. [10].

3.3. Remarks on corner layer terms and on the remainder

Different boundary layer term can interact at *convex* corners of $\partial\Omega$. Then one has to construct *corner layer expansions* Z_M as solutions of elliptic equations in appropiately stretched variables (ζ_1, ζ_2) such that $u_M^{as} = U_M + V_M + Z_M$ satisfies (2). We omit details. In general, there appear at corners the same geometrical singularities of the solution as for standard elliptic equations [11], but on $\varepsilon-$dependent scales. The latter problem is avoided if

(H.5) $U_M + V_M + Z_M \in W^{l+1,\infty}(\Omega)$

which implies certain *data compatibility conditions* (of higher order) at corners. Then the corner layers are essentially tensor products of the interacting layer terms.

The simplest case appears for *diffusion–reaction* problems. The influence of corner layers (and singularities) is then only restricted to a $0(\sqrt{\varepsilon}|\log\varepsilon|)$-region of a corner. For a detailed discussion of this problems (including the case of geometrical singularities and of concave corners) we refer to [12], [14]. The remainder r_M is shown to be smooth and small.

The situation is more complicated for *advection–diffusion-(reaction) problems.* In general, the effect of corner layers is *not local* in corner regions. Singularities of the solution caused by geometrical reasons at points P of $\overline{\Gamma_-}$ are distributed along subcharacteristics of the limit operator L_0 passing through P. Estimates of the remainder r_M are again more complicated. For the simplest case of outflow layers in the unit square only, we refer to the discussion in [6]. A more general result is open so far.

4. Anisotropic Layer Refinement and Interpolation

An *isotropic resolution* is in general to expensive due to the lower-dimensional character of layer phenomena, an *anisotropic* approach is much better suited. This approach is rather new in the literature and far away from being complete [6], [20], [21]. We consider in the special situation of Section 3 some aspects of

such an approach in the special case of *exponential boundary layers* occuring at edges of a convex polygon Ω. The ingredients are the construction of *layer adapted* grids and the (anisotropic) interpolation of boundary layer functions together with the design of the parameters δ_K and γ_K.

4.1. A-priori generation of layer-adapted grids

Let h be a user-given *global* mesh size which is a-priorily set to resolve the solution away from layers. The following steps of the *a-priori* generation of hybrid grids are proposed:

- Detection of boundary layers at an edge $\Sigma \subset \partial\Omega$ and of its width a_Σ
- Generation of a *structured (possibly anisotropic)* mesh in the layer strip $\mathcal{U}(\Sigma)$ of thickness $\mathcal{O}(a_\Sigma)$
- Generation of an (possibly unstructured) *isotropic* mesh of size $h_{1,K} \sim h_{d,K} \sim \mathcal{O}(h)$ away from layer regions.

To be more precise, we discuss the simplified situation of Section 3 with $a_\Sigma \leq h$.

EXAMPLE 4.1. Consider at an edge $\Sigma \subset \partial\Omega$ an edge-fitted Cartesian coordinate system (ϕ, ρ) with $\rho := \mathrm{dist}(x, \Sigma)$ and tangential variable ϕ. A boundary fitted layer-adapted mesh is built in the strip $\mathcal{U}(\Sigma)$: $0 \leq \rho \leq a_\Sigma$ as follows (cf. Figure 2): Setting $\rho = \rho_i,\ i = 0, ..., N+1$ with $\rho_0 = 0$ and $\rho_{N+1} \approx a_\Sigma$, we construct a quadrilateral mesh in the strips $\mathcal{U}^{(i)}(\Sigma) : \rho_{i-1} \leq \rho \leq \rho_i$ with corners in the lines $\rho = \rho_i$. Suppose that the resulting grids at $\rho = \rho_i$ consist of isotropic elements of size $0(h)$.

Assuming $\rho_i - \rho_{i-1} \ll h$ (to be verified below), we subdivide each quadrilateral element into two triangles K in such a way that the maximal angle condition (cf. Section 2.2) and the coordinate system condition (cf. Section 4.2 below) are fulfilled. Then set $h_{d,K} \approx \rho_i - \rho_{i-1} = a_K^{(i)} h$ with $a_K^{(i)}$ to be determined later.

REMARK 4.2. (i) The distribution of (anisotropic) strips parallel to Σ is not necessary. But it turns out from numerical experience, that the longest edge of the finite elements has to be carefully orientied with respect to Σ, at least in the neighborhood of characteristic layers.

(ii) The proposed *a-priori construction* of layer-adapted grids simplifies the presentation but it may also be incorporated within an *adaptive method* where the global mesh size h can be modified based on appropriate a-posteriori estimates or error indicators.

4.2. Anisotropic interpolation estimates

The following condition is useful to describe the *orientation* of the layer-adapted grid and to derive interpolation estimates with respect to the edge-fitted Cartesian coordinate system (ϕ, ρ).

COORDINATE SYSTEM CONDITION (2D): *The angle ψ_K between the longest side of element K and the ϕ–axis (of an appropriate fixed Cartesian coordinate system) is bounded by* $|\sin\psi_K| \le Ch_{2,K}/h_{1,K}$.

It is satisfied in the situation of Example 4.1 with respect to the (ϕ,ρ)-system. The following *interpolation result* [2] takes advantage of different directions in K using the multi-index notation

$$\alpha = (\alpha_1,\alpha_2) \in \mathbf{N}_0^2, \qquad |\alpha| := \alpha_1+\alpha_2, \qquad h_K^\alpha := h_1^{\alpha_1}\cdot h_2^{\alpha_2}$$

and derivatives D^α with respect to the $(\phi,\rho)-$ system. Furthermore, we denote by $\tilde{I}_h^{(l)}(\cdot)$ the Lagrangian interpolant in $\tilde{V}_h \subset \tilde{V} := W^{1,2}(\Omega)$.

THEOREM 4.3. *Assume that a finite element $K \in \mathcal{T}_h$ satisfies the maximal angle resp. coordinate system conditions. Furthermore let be $v \in W^{k,p}(K)$, $k \in \{1,...,l+1\}$, $p \in [1,\infty]$ s.t. $p > 2/k$. Then we obtain for fixed $m \in \{0,...,k-1\}$*

$$|v - \tilde{I}_h^{(l)}v|_{m,p;K} \le C \sum_{|\alpha|=k-m} h_K^\alpha |D^\alpha v|_{m,p;K}.$$

In view of Theorem 2.3, we derive an upper bound of the term $Q_{SG}(v-\tilde{I}_h^{(l)}v)$ as in (16) for a smooth function v on a mesh satisfying the coordinate system condition with respect to a fixed coordinate system.

COROLLARY 4.4. *Under the assumptions of Theorem 4.3 we obtain for v with $v|_K \in W^{l+1,\infty}(K)$ for all elements $K \in \mathcal{T}_h$ and with $\eta_v := (I-\tilde{I}_h^{(l)})v$ that*

$$\begin{aligned} Q_{SG}^2(\eta_v) &\le C\sum_K \mathrm{meas}(K) F_K, \\ F_K &= \sum_{|\alpha|=l-1}\sum_{|\beta|=|\gamma|=1} E_{K;\beta,\gamma} h_K^{2(\alpha+\beta)} \|D^{\alpha+\beta+\gamma}v\|_{0.\infty,K}^2, \qquad (31) \\ E_{K;\beta,\gamma} &:= \varepsilon + C_K h_K^{2\gamma} + \delta_K(\varepsilon^2 h_K^{-2\beta} + B_K^2) + Z_K h_K^{2\gamma}. \qquad (32) \end{aligned}$$

PROOF. Theorem 4.3 implies for $\eta_v := (I-\tilde{I}_h^{(l)})v$ with $k = l+1$ and $p=\infty$ that

$$|\eta_v|_{m,2;K}^2 \le C \sum_{|\alpha|=l+1-m} h_K^{2\alpha}\ \mathrm{meas}(K)\ |D^\alpha v|_{m,\infty;K}^2,$$

hence with $E_{K;\beta,\gamma}$ as defined in (32) follows

$$\begin{aligned} Q_{SG}^2(\eta_v) &:= \sum_K \{\varepsilon|\eta_v|_{1,2,K}^2 + \|\sqrt{c}\eta_v\|_{0,2,K}^2 + \delta_K\|\mathbf{b}\cdot\nabla\eta_v\|_{0,2,K}^2 \\ &+ |\delta_K|\ \|-\varepsilon\Delta\eta_v + c\eta_v\|_{0,2,K}^2 + Z_K\|\eta_v\|_{0,2,K}^2\} \\ &\le C\sum_K \sum_{|\alpha|=l-1}\sum_{|\beta|=|\gamma|=1} E_{K;\beta,\gamma} h_K^{2(\alpha+\beta)}\mathrm{meas}(K) \\ &\quad \|D^{\alpha+\beta+\gamma}v\|_{0,\infty;K}. \qquad \square \qquad (33) \end{aligned}$$

REMARK 4.5. For anisotropic interpolation estimates on quadrilateral elements see [1] .

4.3. Interpolation of exponential layer terms

Now we apply the anisotropic estimates to the interpolation of *exponential boundary layer terms* on a layer-adapted grid as discussed in Example 4.1. To be precise, consider the edge-fitted local coordinate system (ϕ, ρ) and let the following *exponential decay* condition be valid:

(ED) For given numbers $\Gamma > 0$, $\sigma \in (0, 1]$, for $|\alpha| \leq l + 1$ and each element $K \in \mathcal{U}(\Sigma)$ holds

$$||D^\alpha v||_{0,\infty;K} \leq C\varepsilon^{-\alpha_d \sigma} \exp\left(-\Gamma\varepsilon^{-\sigma} \mathrm{dist}(K, \Sigma)\right). \tag{34}$$

EXAMPLE 4.6. Condition (ED) is satisfied in advection-diffusion-reaction problems with $|\mathbf{b}| \geq \beta > 0$ on $\mathcal{U}(\Sigma)$ for

- outflow layers with $\sigma = 1$ and $0 < \Gamma < \min_\phi B_{2,0}(\phi)/A_0(\phi)$, cf. Section 3.2.1, and
- simple characteristic layers with $\sigma = 1/2$, $0 < \Gamma < \min_\phi 1/\sqrt{2H(\phi)}$, cf. Section 3.2.2 (ii).

Furthermore, condition (ED) is fulfilled for layers in diffusion-reaction problems with $\sigma = 1/2$ and $0 < \Gamma < \min_\phi B_{0,0}(\phi)/A_0(\phi)$, cf. Section 3.2.2 (i).

(ED) implies that $||D^\alpha v||_{0,\infty,K} \leq C\varepsilon^{\sigma_0}$ if $\mathrm{dist}(K, \Sigma) \geq \{\sigma(l+1)+\sigma_0\}\Gamma^{-1}\varepsilon^\sigma |\log\varepsilon|$ with $\sigma_0 \geq 0$. The r.h.s. value may be defined as the layer thickness a_Σ. Using an appropriate cut-off function, we suppose that the layer term v vanishes in $\Omega \setminus \mathcal{U}(\Sigma)$. Then we have the following global interpolation estimate:

LEMMA 4.7. *Let a layer-adapted grid be constructed in $\mathcal{U}(\Sigma)\cap\Omega$ as in Example 4.1 with (possibly anisotropic) elements K with $h_{1,K} = \mathcal{O}(h)$ and $h_{2,K} = a_K h$, $a_K \geq \varepsilon^\sigma$. Suppose that a boundary layer term $v \in W^{l+1,\infty}(\Omega)$ satisfies (ED). Then we obtain for the interpolation error $\eta_v := (I - \tilde{I}_h^{(l)})v$ that (with $E_{K;\beta,\gamma}$ defined in (32))*

$$Q_{SG}^2(\eta_v) \leq C \sum_K h^{2l+2} F_K G_K, \tag{35}$$

$$F_K := \sum_{|\beta|=|\gamma|=1} a_K^{1-2\gamma_2} E_{K;\beta,\gamma},$$
$$G_K := \exp\left(-2\Gamma\varepsilon^{-\sigma}\mathrm{dist}(K, \Sigma)\right)\left(a_K\varepsilon^{-\sigma}\right)^{2(l+1)}. \tag{36}$$

PROOF. Corollary 4.4, condition (ED) and the special mesh construction imply

$$Q_{SG}^2(\eta_v) \quad \leq \quad C \sum_K \mathrm{meas}(K) \sum_{\substack{|\alpha|=l-1 \\ |\beta|=|\gamma|=1}} E_{K;\beta,\gamma} h_K^{2(\alpha+\beta)} ||D^{\alpha+\beta+\gamma} v||_{0.\infty,K}^2$$

$$
\begin{aligned}
&\leq C \sum_K \sum_{\substack{|\alpha|=l-1 \\ |\beta|=|\gamma|=1}} E_{K;\beta,\gamma} h^{2(\alpha_1+\beta_1)+1} (a_K h)^{2(\alpha_2+\beta_2)+1} \times \\
&\qquad \times \varepsilon^{-2\sigma(\alpha_2+\beta_2+\gamma_2)} \exp\left(-2\Gamma\varepsilon^{-\sigma}\mathrm{dist}(K,\Sigma)\right) \\
&\leq C \sum_K h^{2l+2} \exp\left(\frac{-2\Gamma\mathrm{dist}(K,\Sigma)}{\varepsilon^\sigma}\right) \left(\frac{a_K}{\varepsilon^\sigma}\right)^{2(l+1)} \times \\
&\qquad \times \sum_{|\beta|=|\gamma|=1} a_K^{1-2\gamma_2} E_{K;\beta,\gamma}. \qquad \square
\end{aligned}
$$

The idea now is to use G_K for an appropriate choice of a_K and to minimize the expression F_K with respect to δ_K (resp. γ_K).

DEFINITION 4.8. *A layer-adapted mesh in the strip $\mathcal{U}(\Sigma) \cap \Omega$ as constructed in Sec 4.1 and satisfying $\sup_K G_K \leq 1$ (with G_K as in (36)) is called* layer-resolvent.

EXAMPLE 4.9. Condition $G_K \leq 1$ can be satisfied recursively (with increasing i) if for all elements K in the strip $\mathcal{U}^{(i)}(\Sigma)$, i.e. $\rho_{i-1} \leq \rho := \mathrm{dist}(K,\Sigma) \leq \rho_i$, holds

$$
a_K^{(i)} := \frac{h}{h_{d,K}} = \frac{\rho_i - \rho_{i-1}}{h} \leq \varepsilon^\sigma \exp\left(\frac{\Gamma\rho_{i-1}}{\varepsilon^\sigma(l+1)}\right). \tag{37}
$$

In particular, in the strip $\mathcal{U}^{(1)}$ nearest to Σ, one has to take $a_K = a_K^{(1)} \approx \varepsilon^\sigma$. One should of course set the values $a_K^{(i)}$ in (37) as large as possible, i.e.

$$
a_K^{(i)} := \frac{\rho_i - \rho_{i-1}}{h} \approx \varepsilon^\sigma \exp\left(\frac{\Gamma\rho_{i-1}}{\varepsilon^\sigma(l+1)}\right). \tag{38}
$$

Setting formally $\Gamma = 0$, hence $a_K \equiv a_K^{(i)} \approx \varepsilon^\sigma$, we get a so-called *Shishkin type* mesh. The number of anisotropic layers $\mathcal{U}^{(i)}$ is then given by $N \sim (l+1)h^{-1}|\log\varepsilon|$, hence the number of (anisotropic) elements in the layer $\mathcal{U}(\Sigma)$ is of order $\mathcal{O}(h^{-2}|\log\varepsilon|)$. Such meshes take no advantage of the exponential decay of layer functions. A mesh satisfying (38) with $\Gamma > 0$ leads to a logarithmically graded mesh of so-called *Gartland type* . The number of layer strips $\mathcal{U}^{(i)}$ is considerably smaller than for a Shishkin mesh. $\square$

THEOREM 4.10. *Let the assumptions of Lemma 4.7 be valid. Furthermore let the mesh be layer-resolvent. With the choice*

$$
|\gamma_K| \leq \delta_K \approx \min\left(h_{2,K} B_K^{-1}; h_{2,K}^2 \varepsilon^{-1}\right) \tag{39}
$$

we obtain

$$
\begin{aligned}
Q_{SG}^2(\eta_v) &\leq C \sum_K h^{2l+2} \frac{h_{1,K}}{h_{2,K}} (\varepsilon + B_K h_{2,K} + C_K h_{2,K}^2) &(40)\\
&\leq C h^{2l} |\log\varepsilon| \max_K \left(\varepsilon^{1-\sigma} + B_K h + C_K h h_{2,K}\right). &(41)
\end{aligned}
$$

PROOF. Starting from Lemma 4.7, we estimate different terms of F_K separately:

$$\sum_{|\beta|=|\gamma|=1} a_K^{1-2\gamma_2} \sim \frac{h_{1,K}}{h_{2,K}}, \quad \sum_{|\beta|=|\gamma|=1} h_K^{2\gamma} a_K^{1-2\gamma_2} \sim h_{1,K} h_{2,K},$$
$$\sum_{|\beta|=|\gamma|=1} h_K^{-2\beta} a_K^{1-2\gamma_2} \sim \frac{h_{1,K}}{h_{2,K}^3}.$$

This implies using (H.2)(i)

$$\sum_{|\beta|=|\gamma|=1} E_{K;\beta,\gamma} a_K^{1-2\gamma_2} \le C \frac{h_{1,K}}{h_{2,K}} E_K; \; E_K := \varepsilon + C_K h_{2,K}^2 + \delta_K B_K^2 + Z_K h_{2,K}^2. \quad (42)$$

We proceed now with the minimization of E_K with respect to δ_K as in the proof of Theorem 2.4. Finally, for the aspect ratio holds $\frac{h_{1,K}}{h_{2,K}} \le \varepsilon^{-\sigma}$. The number of elements is bounded by $h^{-2}|\log\varepsilon|$. □

REMARK 4.11. (i) The interpolation estimate of Theorem 4.10 is of order l and almost uniformly valid with respect to ε. As a remedy, one can consider the original Shishkin mesh with $a_\Sigma \approx \varepsilon^\sigma |\log h|$. This case can be found in [6] for $l = 1$ and $l \ge 1$ in [1]. Furthermore, note that there is a gap of $\mathcal{O}(\varepsilon^\sigma)$ in the first r.h.s. term of (41) as compared to estimates of smooth solutions away from the layer region (cf. Theorem 2.4).
(ii) Condition (39) indicates that the numerical diffusion parameters γ_K and δ_K have to be chosen much smaller in the boundary layer region as compared to the global domain (cf. Theorem 2.4). In particular, we have on a Shishkin type mesh $h_{d,K} \approx \varepsilon^\sigma h$. This implies for advection-diffusion problems with $|B_K| \ge \beta > 0$ for all elements $K \in \mathcal{U}(\Sigma)$ that

- in outflow layers (cf. Section 3.2.1): $|\gamma_K| \le \delta_K \approx \varepsilon h \min(B_K^{-1}; h) \approx \varepsilon h^2$,
- in the simplest characteristic layers (cf. Section 3.2.2): $|\gamma_K| \le \delta_K \approx h \min(\sqrt{\varepsilon} B_K^{-1}; h)$.

A straightforward calculation yields

COROLLARY 4.12. *The estimate of Theorem 4.10 remains valid if we add to a layer term v satisfying (ED) a function $w \in W^{l+1,\infty}(\Omega)$ with $||D^\alpha w||_{0,\infty,\Omega} \le C \ne C(\varepsilon)$ for all $|\alpha| \le l+1$, e.g. the global part U_M of an asymptotic expansion of solution u (cf. Section 3.1).*

4.4. Condensed grids at corners

A condensed mesh (not necessarily of isotropic type) appears if different layer adapted regions $\mathcal{U}(\Sigma_i)$ match at a convex corner $\mathcal{S} = \Sigma_1 \cap \Sigma_2$. Special layer terms compensate perturbations arising around $\mathcal{S}$ from the interacting layers terms. According to (H.5), we neglect here a (possible) singular behaviour of the solution caused by data incompatibility at $\mathcal{S}$. The resolution of geometrical singularities in reaction-diffusion problems is considered in [1].

Let us, without loss of generality, assume that the Cartesian coordinate system (x_1, x_2) is adapted to $\mathcal{S}$ such that the edges Σ_1, Σ_2 are located at $x_s = 0,\ s = 1, 2$. Furthermore, assume that a layer term z satisfies at $\mathcal{S}$ the following exponential decay condition:

(EDC) For given numbers $\Gamma_s > 0,\ \sigma_s \in (0, 1],\ s = 1, 2$, for $|\alpha| \leq l + 1$ and each element $K \in \mathcal{U}(\mathcal{S}) := \mathcal{U}(\Sigma_1) \cap \mathcal{U}(\Sigma_2)$ holds

$$\|D^\alpha z\|_{0,\infty;K} \leq C \prod_{s=1}^{2} \varepsilon^{-\alpha_s \sigma_s} \exp\left(-\Gamma_s \varepsilon^{-\sigma_s} \operatorname{dist}(K, \Sigma_s)\right) \tag{43}$$

which implies certain *data compatibility conditions* at $\mathcal{S}$ to guarantee $z \in W^{l+1,\infty}(\mathcal{U}(\mathcal{S}))$.

EXAMPLE 4.13. Condition (EDC) is satisfied for intersecting outflow/ outflow layers resp. outflow/ characteristic layers with numbers σ_s and Γ_s as in Example 4.6.

Suppose again that, using suitable cut-off functions, the layer term z vanishes in $\Omega \setminus \mathcal{U}(\mathcal{S})$. A straightforward calculation (using similar arguments as in the proof of Theorem 4.10) yields

COROLLARY 4.14. *Suppose that a corner layer term z satisfies (EDC). Then the result of Theorem 4.10 remains valid (with obvious modifications). Note that $h_{2,K}$ has to be choosen according to the layer $\mathcal{U}(\Sigma_s)$ with maximal σ_s.*

REMARK 4.15. A detailed calculation shows that the result of Corollary 4.14 for corner layer terms with (43) remains valid if we add a smooth function (as in Corollary 4.12) and exponentially decaying layer terms (according to Lemma 4.7 and Theorem 4.10) on a condensed mesh at corners of an edge Σ as discussed in Example 4.1.

4.5. Summary

We summarize the results of Section 3, 4 in the following

THEOREM 4.16. *Suppose that the assumptions (H.1)-(H.3) for problem (1)-(2) on the convex polygonal domain Ω are valid. Let an asymptotic expansion (24) be constructed with a smooth regular part U_M as in (H.4) and with boundary resp. corner layer corrections V_M resp. Z_M satisfying (H.5) and the decay conditions (ED) resp. (EDC). Suppose that the remainder r_M satisfies $\|r_M\|_{W^{l+1,\infty}(\Omega)} \leq C \neq C(\varepsilon)$. Then we obtain on a hybrid mesh as constructed in Example 4.1 with layer-resolvent anisotropic refinement according to Def. 4.8 that*

$$|||u - U_h|||_{SG}^2 \leq C h^{2l} |\log \varepsilon| \max_K \left(\varepsilon^{1-\tilde{\sigma}} + B_K h + C_K h h_{2,K}\right). \tag{44}$$

$\tilde{\sigma}$ is the maximal number σ_s which appears in (ED) resp. (EDC).

5. Non-Overlapping Domain Decomposition

We propose a *non-overlapping* domain decomposition method (DDM) for an efficient solution of the arising large discrete systems.

5.1. Continuous problem

Let us consider first the continuous problem (1)-(2). The *idea* of the non–overlapping DDM, on a partition $\overline{\Omega} = \cup_{m=1}^{M} \overline{\Omega}_m$, is to enforce (in appropriate trace spaces) continuity of the solution u and of the flux $\varepsilon \nabla u \cdot \mathbf{n}_{mj}$ at the interfaces $\Gamma_{mj} := \partial\Omega_m \cap \partial\Omega_j$ using a transmission condition of Robin type. More precisely, the iteration for $n \in \mathbf{N}$ consists of solving on Ω_m, $m = 1, ..., M$ (in parallel) the following subproblems:

$$L_\varepsilon u_m^n = f \ \text{ in } \ \Omega_m; \qquad u_m^n = 0 \quad \text{on } \ \partial\Omega_m \cap \partial\Omega \tag{45}$$

together with the *interface conditions*

$$\varepsilon \frac{\partial u_m^n}{\partial \mathbf{n}_{mj}} + \rho_{mj} u_m^n = \varepsilon \frac{\partial u_j^{n-1}}{\partial \mathbf{n}_{mj}} + \rho_{mj} u_j^{n-1} \ \text{ on } \Gamma_{mj} := \partial\Omega_m \cap \partial\Omega_j, \ \ j \neq m. \tag{46}$$

The main problem is the *design* of the functions ρ_{mj} in (46). It turns out that the behaviour of the subcharacteristics of the reduced first order operator L_0 at Γ_{mj}, i.e. the scalar product $\mathbf{b} \cdot \mathbf{n}_{mj}$, is essential. The following class of conditions with arbitrary $\lambda > 0$ is considered

$$\rho_{mj} := \frac{1}{2} \left(-\mathbf{b} \cdot \mathbf{n}_m j + Z_m \right); \quad Z_m = Z_j := \sqrt{(\mathbf{b} \cdot \mathbf{n}_{jm})^2 + 4\varepsilon\lambda}. \tag{47}$$

In [16], [18] we proved the following

Theorem 5.1. *Let (H.1) be valid. Then the solutions of the non–overlapping DDM (45)-(47) converge under appropriate smoothness conditions on the initial guess* u_m^0

$$u_m^n \to u|_{\Omega_m} \ \ \textit{in} \ \ H^1(\Omega_m), \quad n \to \infty.$$

Furthermore we obtain convergence of the traces of $u_m^n - u$ *resp.* $\varepsilon \nabla (u_m^n - u) \cdot \mathbf{n}_m$ *to zero in* $H^{1/2}(\partial\Omega_m)$ *resp.* $H^{-1/2}(\Gamma_{mj})$ *for* $m, j = 1, ..., M, m \neq j$.

Remark 5.2. Different variants of the interface condition (46)–(47) were proposed in recent papers, cf. [16] for a review. In contrast to other methods, our approach allows the field $\mathbf{b}$ both to vanish (Poisson problem or reaction-diffusion problems) or to be parallel to Γ_{mj}.

Theorem 5.1 gives no information on the *convergence rate* of the method. The analysis of a one-dimensional model problem can be found in [16].

5.2. Discrete problem

We consider now a *discrete DDM-version* using the *stabilized Galerkin method* (8)-(10). Let $\mathcal{T}_h$ be an admissible triangulation of the domain Ω with simplicial elements K such that each subdomain Ω_m is the union of such elements K. Further let $V_h \subset V := W_0^{1,2}(\Omega)$ be the subspace with piecewise linear finite elements ($l = 1$). Denote by $B_{SG}^m(\cdot,\cdot)$ and $L_{SG}^m(\cdot)$ the obvious restrictions of $B_{SG}(\cdot,\cdot)$ resp. $L_{SG}(\cdot)$ to Ω_m.

The *discrete DDM* consists in the iterative solution (for $n \in \mathbf{N}$) (in parallel) of the subproblems on Ω_m: *Find* $U_m^n \in V_h^m := V_h|_{\Omega_m}$ *s.t.*

$$B_{SG}^m(U_m^n, v_h) + \sum_{j(\neq i)} \left(\rho_{mj} U_m^n - \Lambda_{jm}^{n-1}, v_h\right)_{\Gamma_{mj}} = L_{SG}^m(v_h)\ \forall v_h \in W_h^m \quad (48)$$

$$\Lambda_{mj}^n := (\rho_{mj} + \rho_{jm})\, U_m^n - \Lambda_{jm}^{n-1} \equiv Z_m U_m^n - \Lambda_{jm}^{n-1} \quad (49)$$

where the explicit calculation of the fluxes is avoided.

Numerical 2D- and 3D-experiments [16], [18] show linear convergence of the discrete DDM independent of h in the full range from advection and/ or reaction–dominated to diffusion–dominated problems. The convergence rate improves with $\varepsilon \to 0$. A typical anisotropic advective transport phase from subdomain to subdomain is observed in the advection–dominated case, otherwise a global isotropic diffusive–reactive transport appears. The overall convergence depends on the number of subdomains. Hence in the massively parallel case one should include some coarse grid solver mechanism.

5.3. Numerical results

The *goal* is now to support the theoretical results by numerical examples using the proposed domain decomposition and the GLS approach. Let be $\Omega = (0,1)^2$ and suppose that boundary layers with thickness a_1 resp. a_2 are located at $\Sigma_1 := \{0\} \times (0,1)$ resp. $\Sigma_2 := (0,1) \times \{0\}$.

The domain is decomposed into the non-overlapping subdomains $\Omega_1 := (a_1,1) \times (a_2,1)$, $\Omega_2 = \mathcal{U}(\Sigma_1) := (0,a_1) \times (a_2,1)$, $\Omega_3 = \mathcal{U}(\Sigma_2) := (a_1,1) \times (0,a_2)$ and $\Omega_4 = \mathcal{U}(\mathcal{S}) := (0,a_1) \times (0,a_2)$. The degenerated case $a_1 = 0$ is allowed. We choose $a_i = C\varepsilon^{\sigma_i}|\log\varepsilon|$ as the layer thickness. The main reason is to keep the fluxes appearing in the interface condition uniformly bounded with respect to ε.

Each subdomain is now assigned to a processor of a multi-processor system. Note that the resolution of the boundary layer and corner layer regions according to Section 4 guarantees an appropriate load balancing. The resulting discrete problems are solved using the preconditioned QMRCGSTAB method.

5.3.1. Outflow layers

We consider first the more academic case of outflow layers in advection-diffusion problems.

EXAMPLE 5.1. Consider problem (1)-(2) with $\mathbf{b} = -(1,1)^T, c = 0$ and the exact solution

$$u = \sum_{i=1}^{2} \exp(-x_i/\varepsilon) - \prod_{i=1}^{2} \exp(-x_i/\varepsilon)$$

with vanishing global expansion U_M and outflow layers at $x_1 = 0$ and $x_2 = 0$. The corner layer term $\prod_{i=1}^{2} \exp(-x_i/\varepsilon)$ can be resolved by the condensed mesh at the origin. The remainder of the asymptotic expansion vanishes.

The domain decomposition is performed with $a_1 = a_2 = 2\varepsilon|\log\varepsilon|$. Application of Theorem 4.10 to the outflow layers and Corollary 4.14/ Remark 4.15 to the corner layer yield the global (and almost uniform with respect to ε) estimate

$$|||u - U_h|||_{SG}^2 \leq Ch^2|\log\varepsilon|.$$

We resolve the outflow layers by a Shishkin type mesh. In Figure 3 we present the convergence history in the energy norm and L^2-norm for $\varepsilon = 10^{-3}$ and different choices of $\delta_{loc} \equiv \delta_K = \gamma_K$ in the layer elements. First resp. second order accuracy are observed. On the other hand, for moderate h, the error is considerably smaller for $\delta_{loc} = 0$ and $\delta_{loc} = \varepsilon h^2$ in comparison to $\delta_{loc} = Ch$ which would be the standard choice on an isotropic mesh. This supports Remark 4.11 (ii). There is no remarkable difference between the seq(uential) and the DD solutions.

5.3.2. Characteristic layers
Consider now the case of characteristic edge(s).

(i) Reaction-diffusion problems: (cf. Section 3.2.2 (i))

EXAMPLE 5.2. Consider problem (2)-(2) with $\mathbf{b} = (0,0)^T, c = 1$ and the exact solution

$$u = \exp(-x_1/\sqrt{\varepsilon}) + \exp(-x_2/\sqrt{\varepsilon})$$

which consists s only of two exponential boundary layer terms.

The domain decomposition is performed with $a_1 = a_2 = 2\sqrt{\varepsilon}|\log\varepsilon|$. Application of Theorem 4.10, Corollary 4.14 and Remark 4.15 result in

$$|||u - U_h|||_{SG}^2 \equiv |||u - U_h|||_G^2 \leq Ch^2\sqrt{\varepsilon}\,|\log\varepsilon|$$

which is uniformly valid with respect to ε. In Figure 4 we present the convergence history in the energy norm (unscaled and scaled) for a Shishkin type mesh and different values of ε. We observe similar results as in Example 5.1 and additionally robustness with respect to ε. Furthermore, the scaled results (energy norm divided by $\sqrt{\varepsilon^{1/2}|\log\varepsilon|}$) indicate that this factor in the theoretical estimate is sharp.

Now we compare the layer resolution with a Shishkin and a Gartland type mesh on moderate fine meshes with $65 \times 65 = 4225$ resp. $43 \times 43 = 1849$ grid

ε	mesh type	energy norm	L^2–norm	L^∞–norm
10^{-2}	Shishkin	6.430E-003	2.234E-004	1.413E-003
	Gartland	1.560E-002	8.072E-004	5.406E-003
10^{-6}	Shishkin	1.711E-003	1.500E-004	8.659E-003
	Gartland	2.254E-003	4.191E-004	2.132E-002
10^{-10}	Shishkin	2.842E-004	2.639E-005	2.043E-002
	Gartland	2.681E-004	3.101E-005	1.511E-002

TABLE 1. Comparison of Shishkin and Gartland type grids in Example 5.2

points. The error is nearly of the same order on both meshes (at least for small ε), cf. Table 1. The Gartland type mesh should be prefered due to the smaller number of required (anisotropic) elements.

(ii) Advection-diffusion problems: Let us consider the simplest case of a non-degenerating characteristing layer with $k_1 = 0, k_2 \geq 2$ in (29) (cf. Section 3.3.2 (ii)).

EXAMPLE 5.3. Consider problem (1) with $\mathbf{b} = (1,0)^T, c = 0$ and the exact solution

$$u = \frac{1}{\sqrt{1+x_1}} \exp\left(-\frac{x_2^2}{4\varepsilon(1+x_1)}\right)$$

with a parabolic layer term at $x_2 = 0$, hence $a_1 = 0$. No global and corner layer terms appear. The error estimate follows from Theorem 4.10

$$|||u - U_h|||_{SG}^2 \leq Ch^2(\sqrt{\varepsilon} + h)|\log\varepsilon|.$$

In Figure 5 we compare the convergence history in the energy norm and L^2-norm for $\varepsilon = 10^{-6}$ and different choices of the parameters $\delta_{loc} \equiv \delta_K = \gamma_K$ in the layer region with resp. without domain decomposition (seq. resp. DD). Again we obtain first resp. second order convergence for the energy resp. the L^2-norm. The first observation is that the choice $\delta_{loc} \approx h$ is somewhat better than the variants with a much smaller δ_{loc}. This supports again Remark 4.11(ii). Furthermore, the domain decomposition approach with $\delta_{loc} \approx h$ is seemingly more stable as the discrete solvers had problems for small values of h in the sequential case.

6. CONCLUDING REMARKS

In this paper, we consider error estimates (in the energy norm) for stabilized Galerkin methods. After a review of such methods on isotropic meshes we focus the discussion on the *a–priori resolution* of boundary layers. The main point is a refined design of critical discretization parameters which depend on the diameter of the largest ball inscribed in an element K.

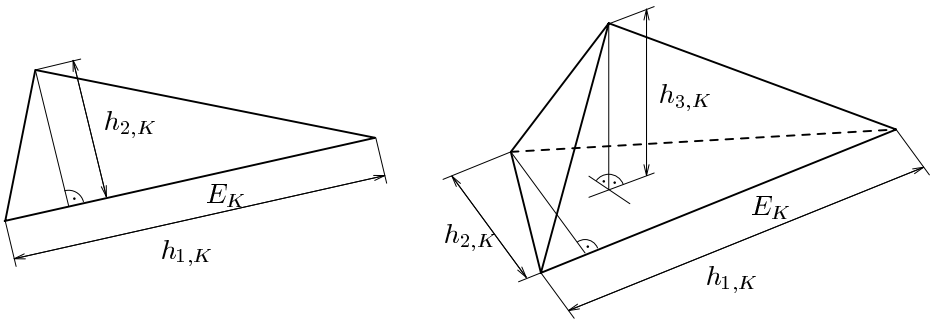

FIGURE 1. Element related mesh sizes.

The analysis is based on anisotropic interpolation estimates of different layer parts of the asymptotic expansion of the solution. This has been done for the special (but important) case of exponentially decaying boundary layers appearing at edges of an polygonal domain $\Omega \subset \mathbf{R}^2$. Furthermore, we discuss different types of layer-resolvent grids. Meshes of Shishkin type, recently introduced in the literature, are covered. Grids which are more adapted to the exponential decay of the layer (e.g. of Gartland or Bachvalov type) require much less grid points in the layer and give essentially the same numerical results. Numerical results for different exponential layer types confirm the theoretical convergence rate for the energy norm l (here $l = 1$). A theoretical foundation of the observed second order convergence rate (for $l = 1$) in the L^p-norms will be considered elsewhere.

A remarkable fact is that numerical diffusion parameters of the stabilized Galerkin methods have to be chosen much smaller in layer regions than predicted by the theory on isotropic meshes. However, it is preferable to stabilize the Galerkin method (at least away from layers) in order to get a robust discrete problem.

Open problems are the discussion of more complicated layers, the extension to curved manifolds generating the layers and to interior layers. Other important topics are the resolution of geometrical singularities and estimates of the remainder of the asymptotic expansion which will be discussed elsewhere.

The proposed *a-priori approach* to the resolution of boundary layers is of course more or less academic and restricted to problems with a known asymptotic structure of the solution. In more realistic problems (nonstationary and/or nonlinear – with possibly moving interior layers), an *adaptive approach* is necessary. Ingredients of such a method would be sharp a-posteriori estimates for singularly perturbed problems (cf. [25]) and an adaptive method which allows anisotropic refinement (cf. e.g. [23]).

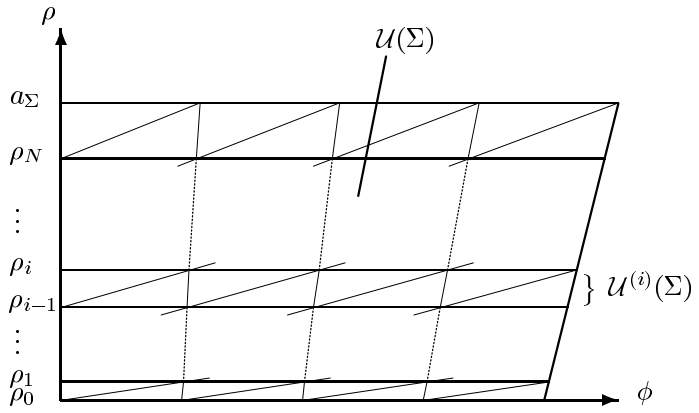

FIGURE 2. Adapted grid in a boundary layer strip

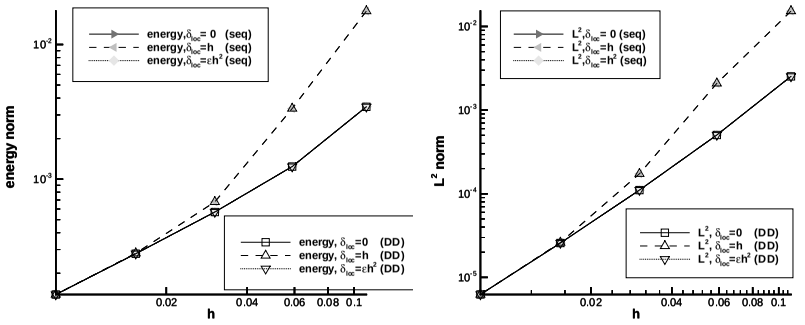

FIGURE 3. Convergence in the energy and L^2-norms for Example 5.1 on a Shishkin mesh

REFERENCES

1. APEL, TH. *Anisotropic finite elements: Local elements and applications.* Habilitation Thesis, TU Chemnitz-Zwickau (in preparation)
2. APEL, TH., LUBE, G. (1997). Anisotropic mesh refinement for singularly perturbed reaction-diffusion problems. *Appl. Numer. Math.* **26**, 1–19.
3. APEL, TH., LUBE, G. (1996). Anisotropic mesh refinement in stabilized Galerkin methods. *Numer. Math.* **74**, 262–282.
4. CODINA, R. (1993). A discontinuity-capturing crosswind-dissipation for the finite element solution of the convection-diffusion equation. *Comp. Meths. Appl. Mech. Engrg.* **110**, 325–342

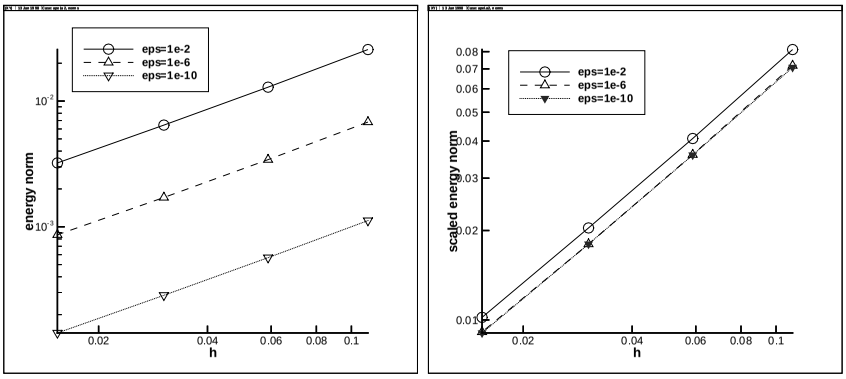

FIGURE 4. Energy norm convergence (unscaled/ scaled) for Example 5.2 on a Shishkin mesh

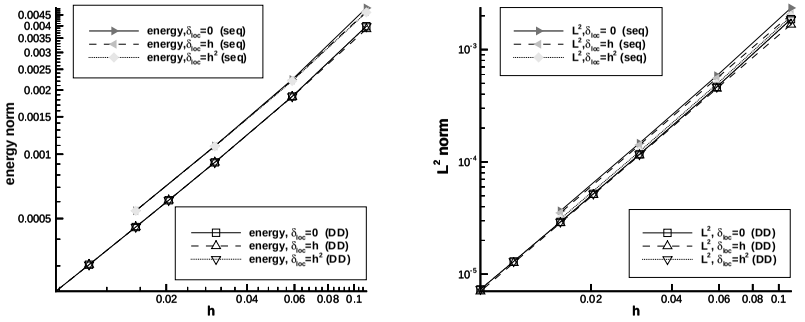

FIGURE 5. Convergence in the energy and L^2-norms for Example 5.3

5. CODINA, R., BLASCO, J. (1997). *Analysis of a finite element approximation of the stationary Navier-Stokes equations using equal order velocity-pressure interpolation.* Preprint CIMNE No. 113, Barcelona (submitted to SINUM)
6. DOBROWOLSKI, M., ROOS, H.-G. (1997). A-priori estimates for the solution of convection-diffusion problems and interpolation on Shishkin meshes. *ZA* **16**, 4, 1–13.
7. FARHAT, C., FRANCA, L.P. (1995). Bubble functions prompt unusual stabilized finite element methods. *Comp. Meths. Appl. Mech. Engrg.* **123**, 299–308.
8. FRANCA, L.P., DUTRA DO CARMO, E.G. (1989). The Galerkin gradient least-squares method. *Comp. Meths. Appl. Mech. Engrg.* **74**, 41–54.
9. FRANCA, L.P., FREY, S.L., HUGHES, T.J.R. (1992). Stabilized finite

element methods: I. Application to the advective-diffusive model. *Comp. Meths. Appl. Mech. Engrg.* **95**, 253–276
10. Goering, H., Felgenhauer, A., Lube, G., Roos, H.-G., Tobiska, L. (1983). Singularly perturbed differential equations. *Math. Research*, **13**, Akademie-Verlag, Berlin.
11. *Grisvard, P.* (1985). *Elliptic problems in non-smooth domains.* Pitman, Boston.
12. Han, H., Kellog, R.B. (1990). Differentiability properties of solutions of the equation $-\varepsilon^2\Delta u + ru = f$ in a square. *SIAM J. Math. Anal.* **21**, 394–408.
13. Johnson, C., Schatz, A.H.., Wahlbin, L.B. (1984). Crosswind smear and pointwise errors in streamline diffusion finite element methods. *Math. Comput.* **49**, 25–38.
14. Kellog, R.B. (1995). Boundary layers and corner singularities for a self-adjoint problem. *Boundary value problems and integral equations in non-smooth domains* (eds. M. Costabel et. al.), Dekker, New York, 121–149.
15. Lube, G. (1994). *Stabilized Galerkin finite element methods for convection dominated and incompressible flow problems.* Banach Center Public. **29**, Inst. Math., Polish Acad. Sc., Warszawa.
16. Lube, G., Otto, F.-C. (1997). A nonoverlapping domain decomposition method for incompressible flow problems. Appears. in: *Proc. Third Intern. Conf. Numeric. Modelling in Contin. Mech.*, Prague
17. Lube, G., Weiss, D. (1995). Stabilized finite element methods for singularly perturbed parabolic problems. *Appl. Numer. Math.* **17**, 431–459
18. Otto, F.C., Lube, G. A non-overlapping domain decomposition method for the Oseen equations. Appears in M^3AS.
19. Quarteroni, A., Valli, A. (1994). *Numerical approximation of partial differential equations.* Springer.
20. Roos, H.G. *Layer-adapted grids for singular pertubations problems.* Preprint MATH-NM-03-1997, TU Dresden
21. Roos, H.G., Stynes, M., Tobiska, L. (1996). *Numerical methods for singularly perturbed differential equations.* Springer, Heidelberg.
22. Schatz, A.H., Wahlbin, L.B. (1983). On the finite element method for singularly perturbed reaction-diffusion problems in two and one dimensions. *Math. Comput.* **40**, 47–89.
23. Skalicky, T., Roos, H.-G. (1997). *Anisotropic mesh refinement for problems with internal and boundary layers.* Preprint Math-NM- 09-97, TU Dresden, Faculty of Math.
24. Valentin, F., Franca, L.P. (1995). *Combining stabilized finite element methods.* UCD/ CCM Report No. **48**, Denver.
25. Verfürth, R. (1997). *A posteriori error estimates for convection-diffusion equations.* University of Bochum, Faculty of Mathematics, Preprint.